JME

Journal of Mining & Environment,
Vol.3, No.2, 2012, 103-111.

A new approach to define batch settling curves for analyzing the sedimentation characteristics

M.R. Garmsiri[1] , H. Haji Amin Shirazi[2]*

1. *Mining Engineering Group, Young Research Society, Shahid Bahonar University of Kerman, Kerman, Iran.*
2. *Mining Engineering Group, Mineral Industries Research Centre, Shahid Bahonar University of Kerman, Kerman, Iran.*

Received01December2011; received in revised form13February2012; accepted 25December 2012
**Corresponding author: hshirazi@uk.ac.ir(H. H. Amin Shirazi).*

Abstract
The results of batch settling tests (BSTs) are used to investigate the settling behavior of solids suspension, which contribute to sizing thickeners. Conventional methods in analyzing BST on the basis of visual and graphical procedures lead to sub-optimally sized and selected thickeners. A computational approach based on quantitative analysis of BST can be beneficial. About 300 settling experiments were performed by varying conditions including solids concentration, type and dosage of chemical aids. Solid samples were collected from iron, copper, coal, lead and zinc tailings and feed streams. Considering extreme limits, settling curves were generated and analyzed based on experimental data. Therefore, a mathematical model, *h(t)*, is introduced to define batch settling curves. Furthermore, it is shown that, on settling velocity curves a maximum value is likely to occur (except in extreme conditions such as very high or very low solids concentration suspensions or extremely high dosage of flocculant). In addition, based on parameters obtained from the model *h(t)*, an index, I_i, is developed to compare batch settling curves quantitatively. The proposed model and index can simply be utilized in a computerized approach of settling curves analysis.

Keywords: *Solid liquid separation, Thickening, Batch settling test, Mathematical model, Settling velocity*.

1. Introduction

Gravity sedimentation is the most common technique applied for solid-liquid separation, and batch settling tests (BSTs) are used to obtain detailed information of sedimentation behavior (e.g. settling velocity) of suspensions. During the batch settling, the solids pass from free to hindered settling and then to compression conditions. Thus, batch settling consists of two distinct stages: settling and consolidation. With a given initial settling rate and the value of critical point, BSTs have been a major step of sizing thickeners and clarifiers [1-6]. BSTs can also be used in determining dewaterability of sludges. These tests are an important step in estimating compressive yield stress and hindered settling function [7, 8]. Furthermore, choosing appropriate flocculant for operation, the effect of flocculant properties on sedimentation, aggregates properties and generally the effect of impressive factors in settling can be investigated by using BSTs [9-12]. In the last two decades, BSTs have been conducted to study settling process in different areas such as minerals industries [13], waste water treatment [14], filtration [15], sewage [16], drinking water [17], ocean engineering [18], dredging [19], environment [19] and biotechnology [20].

Kynch [2] developed a model to describe batch settling curves (the mudline height vs. time) assuming that the suspension was ideal. This theory was used in thickener sizing by others [3, 4]. He showed that settling velocity depends on local concentration of suspension. This led to a relation between local concentration, time and position, as a partial differential equation (PDE) [Eq. 1].

$$\frac{\partial X}{\partial t} - \frac{\partial f_b(X)}{\partial z} = 0 \quad (1)$$

Where z is the height from the bottom in sedimentation column, $f_b(X) = Xv_s(X)$ is the batch settling flux function, X is volumetric solids concentration and v_s is settling rate.

Modeling of detailed information of the BSTs (especially settling velocity) has been the focus of attention in the last few decades. Vesilind in 1968 on the assumption that, velocity was only dependent on local sludge concentration presented an Eq. (2) [21, 22].

$$V_s(X) = V_0 e^{-nX} \quad (2)$$

Where V_0 and n are model parameters and X is volumetric concentration of solids.

Takács et al. [23] and Cho et al. [24] presented Eqs. (3) and (4) respectively.

$$V_s(X) = V_0^{'}(e^{-r_h(X_j - X_{min})} - e^{-r_p(X_j - X_{min})}) \quad (3)$$

$$V_s(X) = k^{'}(\frac{e^{-n^{'}X}}{X}) \quad (4)$$

Where $V_0^{'}$ is maximum theoretical settling velocity, X_j is suspended solids concentration in layer j, X_{min} is minimum attainable suspended solids concentration, r_p settling parameter associated with the low concentration and slowly settling component of the suspension, r_h settling parameter associated with the hindered settling component of settling velocity equation and also X is solids concentration by weight, $k^{'}$ and $n^{'}$ are constant.

Grijspeerdt et al. [25] stated that batch settling data could be well fitted using Takács et al. model. While, Watts et al. [26] asserted that the Takács et al. model could be simplified to the Vesilind model for the estimation of sludge blanket dynamics.

Vanderhasselt and Vanrolleghem [27] compared the Vesilind approach using zone settling velocity (V_{zs}) data and Cho et al. method (direct parameter estimation) relying on a single batch settling curve. They declared that the Vesilind model is superior to the Cho et al. model in describing the relationship between V_{zs} and X (sludge concentration), while the Cho et al. model is better in describing complete settling curves which implies that, current settling models are still very empirical in nature. Furthermore, they concluded that the reliability of Cho et al. flux curve predictions is insufficient to validate replacement of the conventional estimation of settling parameters.

Banisi and Yahyaei [28] proposed Eq. (5) to describe settling curves. However, its efficiency has not been discussed.

$$h(t) = Exp(\frac{a_0 + a_1 \times t + a_2 \times t^2 + \ldots + a_n \times t^n}{1 + b_1 \times t + b_2 \times t^2 + \ldots + b_m \times t^m}) \quad (5)$$

Where $a_0, a_1, \ldots, a_n$, $b_1, b_2, \ldots, b_m$ are model parameters, $h(t)$ is the height of interface and t is settling time.

Focusing on the nonlinear section of the batch settling curves, Grassia et al. [29] indicated that power law and exponential decay functions are reasonable fits to simulated synthetic height vs. time data derived from the settling flux function previously employed by Lester et al. [30]. Furthermore, it was concluded that the parameters of the power law fit to settling curve could be utilized in the analytic formula for settling flux.

In this work, BSTs modeling is investigated varying settling conditions. Detailed analysis of BSTs results are then performed utilizing the developed model. BSTs results were analysed and compared quantitatively utilizing the developed model.

2. Materials and methods

2.1. Batch settling tests

Batch settling experiments of varying conditions as shown in Table 1, were performed using a graduated glass cylinder (500 cm^3; 25.4 cm height and 5 cm diameter or 1000 cm^3; 35.4 cm height and 6.1 cm diameter). The height of the mudline was mostly measured visually, except for high settling rate for which a camcorder was used, and the first measurement was done in 3 seconds after the start of the test. A schematic view of a BST in 600 seconds is illustrated in Figure 1.

Table 1. Batch settling tests conditions

Condition	Description
Samples	Copper, coal and iron tailings and lead and zinc feed samples
Test duration	10-120 min
Pulp solids concentration	2-50 % by weight
pH	7-12
Flocculant type	None ionic, anionic and cationic
Flocculant dosage (g/t)	0-70

Flocculant solutions were made up with concentration of 0.1 g/l and diluted to different concentrations.

In most cases, the slurry was mixed by 3 times inversion (turning the graduated cylinder upside down), whereas a plunger was used infrequently.

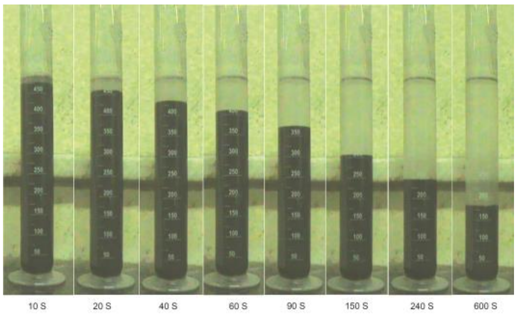

Figure 1.A schematic view of a BST in 600 seconds

2.2. Model adequacy analysis

The adequacy of a model was analyzed considering the coefficients of determination (R^2) and adjusted R^2:

$$SS_E = \sum(y_i - f_i)^2 \tag{6}$$

$$SS_T = \sum(y_i - \bar{y})^2 \tag{7}$$

$$R^2 = 1 - SS_E/SS_T \tag{8}$$

$$R^2_{adj} = 1 - (1 - R^2)\frac{n-1}{n-p-1} \tag{9}$$

Where SS_E is sum of square errors, SS_T is sum of square deviations of the experimental data y_i from their mean $\bar{y}$, f_i is model results, n is sample size and p is total number of regressors in the model[31].

The resulted R^2 is within the range 0-1, while the adjusted R^2 is always less than or equal to R^2 and may be negative. As an advantage over R^2, the number of data points and model variables are taken into account in the adjusted R^2. With these coefficients being closer to 1, the adequacy of a model is improved.

3. Results and discussion

3.1. Model development

Figures 2 and 3 show typical settling curves for various mineral samples, flocculant dosage and particle size.

As illustrated in Figures 2 and 3, the resulted settling curves from all possible combinations of solids concentrations and flocculant dosages is laid between two extreme limits. As indicated, curve *A* resulted from high solids concentration with no flocculant addition, whereas curve *D*, resulted from dilute suspension with high flocculant dosage.

A software (Find Graph 5) was utilized to find potential equations on the basis of a variety of batch settling curves considering extreme limits, such as shown in Figures 2 and 3. As a result, candidates to describe the curves were primarily chosen.

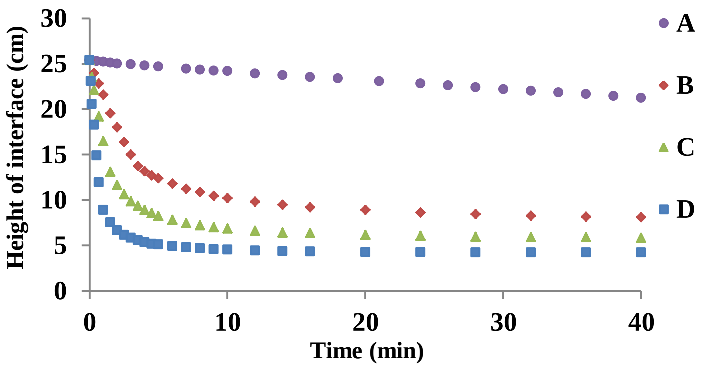

A: 40% solids concentration by weight, no flocculant
B: 15% solids concentration by weight, flocculant dosage 15 g/t
C: 11% solids concentration by weight, flocculant dosage 15 g/t
D: 7% solids concentration by weight, flocculant dosage 15 g/t

Figure 2. Typical settling tests performed using copper tailings in 500 cm^3 cylinder in varying conditions; d_{80}: 107 µm, pH=11, solids density: 2.6 g/cm^3

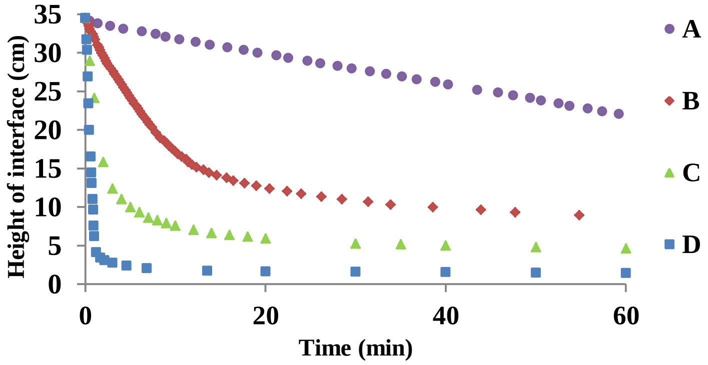

A: Lead & Zinc ore, Solids density: 3.7 g/cm^3, d_{80}: 55 µm, 35% solids concentration by weight, no flocculant
B: Coal tailings, Solids density: 1.6 g/cm^3, d_{80}: 35 µm, 8% solids concentration by weight, flocculant dosage 35 g/t
C: Iron tailings, Solids density: 4 g/cm^3, d_{80}: 63 µm 8% solids concentrations by weight, flocculant dosage 5 g/t
D: Coal tailings, Solids density: 1.6 g/cm^3, d_{80}: 35 µm, 2% solid concentration by weight, flocculant dosage 15 g/t

Figure 3. Typical settling tests performed using different minerals in varying conditions in 1000 cm^3 cylinder:

It was found that about 30 equations might describe the curves [32]. All of the equations chosen in the first step were examined by using the results of a limited number of settling tests. Consequently Eqs. (10-12) were distinguished to be the candidates for further consideration.

$$h(t) = a + b \times Exp(-t/c) + d \times Exp(-t/f) \qquad (10)$$

$$h(t) = a + b \times Exp(-t/c) + d \times Exp(-t/f) + g \times Exp(-t/h) \qquad (11)$$

$$h(t) = Exp(\frac{at^2 + bt + c}{dt^2 + ft + g}) \qquad (12)$$

Where *h(t)* is the height of interface (cm) in desired time, *t* is time (min), *a,b,c,d,f,g,h* are model parameters.

3.2. Model validation

The three equations were fitted on the experimental results of about 300 settling tests as presented in Table 1. At this stage, the verification criteria were considered to be the coefficient of determination (R^2). The results obtained by applying Eqs. (10-12) are shown in Table 2.

Table 2.Coefficient of determination resulted from applying Eqs. (10), (11) and (12) to approximately 300 BSTs of varying conditions

Equation	Results with R^2> 0.998 (%)	Results with R^2> 0.99 (%)	R^2 Mean	R^2 Standard deviation
10	75.9	98.2	0.9983	0.002
11	91.1	99.6	0.9990	0.0011
12	92.6	100	0.9992	0.001

According to Table 2, R^2 values of all of the three equations were more than 0.99 at least in 98% of the cases, which implies that, each of them can be used to define a variety of entire settling curves accordingly. While, using Eqs. (11 and 12), the R^2 values are more than 0.998 in 91.1 and 92.6% of the cases, respectively. This suggests that Eqs. (11 and 12) are the remaining two candidates for further consideration.

In finding the appropriate model, the number of experimental data points should be as great as possible, and the number of model variables should be as few as possible. Thus, to consider the number of data points and model parameters in the chosen equations, the adjusted R^2 values were used as the verification criteria. The results of fitting the three models to the data from the settling tests considering R^2_{adj} are shown in Table 3.

Table 3. Adjusted R^2 resulted from applying Eqs. (10), (11) and (12) to about 300 tests of varying conditions

Equation	Results with R^2_{adj}>0.998 (%)	Results with R^2_{adj}>0.99 (%)	R^2_{adj} Mean	R^2_{adj} Standard deviation
10	74.1	98.2	0.9982	0.0021
11	89.7	99.6	0.9990	0.0011
12	92.2	100	0.9992	0.0010

From the results presented in Table 3, a similar conclusion is confirmed and the Eqs. (11-12) are proved to be acceptable in defining batch settling curves. However, regarding the number of parameters and precision, Eq. (12) is superior. This can be considered as a modified version of the model developed by Banisi and Yahyaei[28].

These models are supposedly suitable to be applied not only in mineral industries for which the results are validated but also in other areas in which BSTs are used to study sedimentation of suspensions. Work is currently underway to analyze the reliability of the results.

3.3. Application of settling models

3.3.1. Critical point estimation

As solids settle in a BSTs, with increasing solids concentration, the settling condition is changed from free to hindered settling and then to compression. Depending on the test condition, the contributions of free settling, hindered settling and compression zone can be different.

A point at which the hindered settling ends and compression zone commences is referred to as compression or critical point. Determining the critical point is essential in some of the thickener sizing methods including Talmage and Fitch [3].

Gupta and Yan [33] reviewed conventional methods; bisecting, Mondal&Mujomdar and log ($H-H_\infty$) which are commonly used to determine the critical point. These methods are based on a graphical procedure and more or less dependent on the personal decision of the analyst. Thus, using a mathematical method to determine the critical point of the settling curves is essential.

During a settling test, as time goes on, (with the condition changing from free to hindered settling), settling rate decreases nonlinearly. Therefore, critical point can be located where the acceleration of the interface displacement approaches to zero. In this study, the second derivative of the settling curve model is suggested to be used in critical point estimation. In practice it is observed that critical point occurs where the second derivative of the model approximates to the value 0.1. The results of the conventional methods and estimated values obtained from second derivative of the Eq. (12) for the curves illustrated in Figure 2 are shown in Table 4.

Table 4. Results of estimating critical point of Figure 2 by different methods

	Critical point (minutes)			
	Bisecting	Mondal&Mujomdar	Log(H-H_∞)	Using second derivation of Eq. (12)
Curve A	Does not work	Does not work	Does not work	38 Seconds
Curve B	6	12	10	7.77
Curve C	4.5	6	5	6.43
Curve D	3	4	2.5	4

As illustrated in Figure 2, Curve (A) corresponds to a high solids concentration suspension which resulted in compression condition in the early seconds of the test. The conventional methods are based on a graphical procedure. Therefore, they are not applicable in determining critical points of settling curves of high solids concentration suspensions such as curve (A) in Figure 2. While, by using the mathematical method, the critical point of the curve (A) was simply found to be after 38 seconds from the start of the test. Furthermore, in the conventional method, the difference between the results of each curve could be attributed to the analyst personal decision. On the other hand, the result of the mathematical method is more reliable since it is independent of the analyst.

3.3.2. Calculating settling velocity

As an important application, BSTs results are used in determination of solids flux, which in turn is utilized in the design and sizing of solid liquid separation equipments. As mentioned earlier, the flux function is directly dependent on the settling rate. The slope of a settling curve is commonly determined by drawing a tangential line to the curve at that point. This procedure is also applied to estimate the initial settling rate of the curve [34-36].

At any point of a settling curve, the first derivative of the developed Eq. (12) can be used to calculate the exact settling velocity of the mudline at that point. Figures 4 and 5 show the change of settling velocity of interface due to the change of solids concentration for the curves shown in Figures 2 and 3, respectively. It is shown that, in some cases a maximum value on the settling velocity curve is observed at the early stage of the test. This is in contrast with Kynch theory which suggests that settling velocity is a function of solids concentration, and can be attributed to the fact that in addition to the solids concentration other factors such as floc density, shape and size of the particles and flocculation quality have an effect on settling velocity [37]. Furthermore, shear and weak flocculation may also result in a maximum value in the settling velocity of the interface.

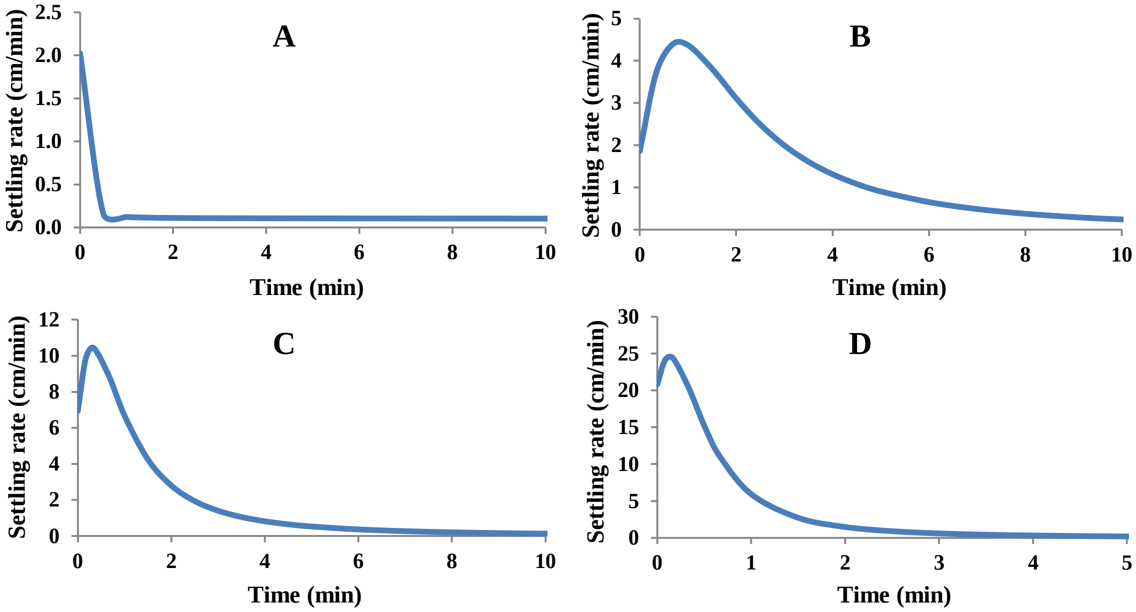

Figure 4. Settling velocity of interface vs. time generated by the first derivation of Eq. (12) corresponding to settling curves shown in figure 2.

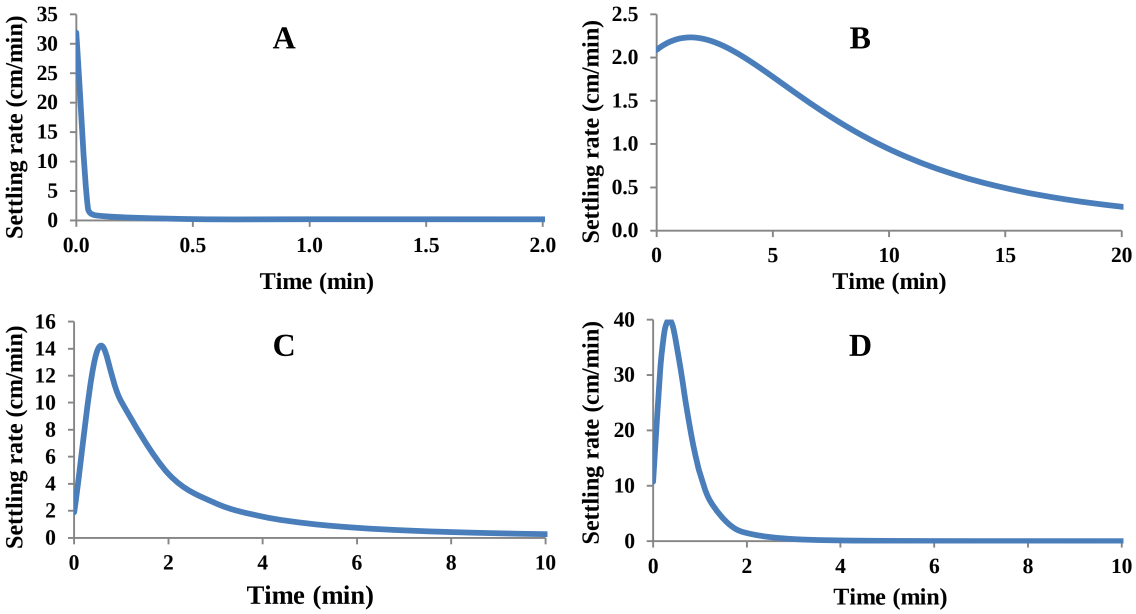

Figure 5. Settling velocity of interface vs. time generated by the first derivation of Eq. (12) corresponding to settling curves shown in figure 3.

Using the mathematical model (Eq. 12), settling velocities of the 300 experiments were examined to predict the consequence of any specific condition. Results showed that, in the most cases during the test, settling velocity rose to a maximum value then declined. While, the maximum velocity was not observed in the cases of high settling velocity (due to high flocculant dosage or extremely dilute pulp) or low settling velocity (due to high solids concentration suspensions with no flocculant addition).

It can be deduced that settling velocity of the interface may increase to a maximum value at the early stage of a settling test. Then, with increasing solids concentration a gradual decrease in settling velocity occurs. However, with high solids concentration suspensions which causes compression condition from the early stage of the test, this phenomenon is not observed.

Referring to Figures 4 and 5, the maximum values on the settling velocity curves have been occurred in very short periods after the start of the tests (approximately in the first 22 seconds). This implies that in most cases the curve reaches the maximum and then declines on the corresponding settling curves in Figures 2 and 3. In practice, by drawing a tangential line to the settling curve the exact initial slope of the curve cannot be detected. In addition, when the slope of the tangential line is high, the *tan* of the degree of the slope changes markedly with slight differences in the degree of the slope, which results in high levels of error in the obtained initial slope of the settling curves. On the other hand, since the direction of the slope of the settling curves may be varied, it must clearly be specified that at which point the first derivative of the *h(t)* is desired.

To estimate the initial slope of a settling curve, Eq. 13 was suggested with the multiplier α equal to 0.05 [38]. In an attempt to verify the results, the initial slope of the 300 settling curves was estimated by using a conventional method (the slope of the trend line between initial data points) and the suggested equation by varying α. The relationship between the results obtained using Eq. 13 versus the common method is shown as a trend line in Figure 6. The R^2 value and the slope of the trend line with varying values of α are shown in Table 5. The estimation can be further improved by considering smaller values of α to a minimum value of 0.029.

$$\text{Initial slope} = \frac{h'(0) + h'(\alpha CPt)}{2} \qquad (13)$$

Where: h' is first derivative of the equation;and *CPt* is Critical point time.

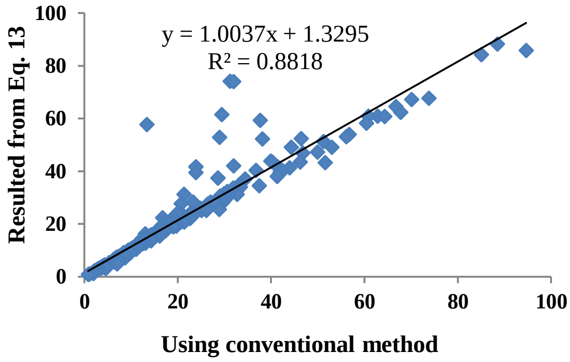

Figure 6. Initial slope resulted from Eq. (13) versus initial slope obtained using conventional method.

Table 5. Verification of the Eq. (13) on the basis of value of α considering R^2 and slope of the trend line between the results

α	R^2	Slope
0.050	0.875	0.883
0.040	0.878	0.933
0.035	0.879	0.962
0.032	0.880	0.982
0.030	0.881	0.996
0.029	0.881	1.003
0.028	0.882	1.011
0.025	0.883	1.034

3.3.3. Comparing settling curves quantitatively

A comparison of the settling curves is of great significance. A visual comparison can only reveal the situation as being better or worse. Initial slope of the curves has mainly been distinguished. However, after a longer time the condition may change. Therefore, a comparison is suggested based on an index defined considering the curves entirely.

An approach based on the definition of a visual comparison of the curves is proposed to perform a quantitative comparison of the settling curves with the goal of a computerised analysis. Curves characteristics including the initial slope of the curve, the height of the interface of the clear water, and suspension at different times are considered. For a relative comparison of the settling curves, an index I is introduced (Eq. 14).

$$I_i = K \times \frac{S_i}{\overline{S}} \times \frac{\overline{h_{20}}}{h_{20i}} \times \frac{\overline{h_{60}}}{h_{60i}} \times \frac{\overline{h_c}}{h_{ci}} \qquad (14)$$

Where

I_i is the index amount of i^{th} curve

S_i is the initial slope of i^{th} curve

$\overline{S}$ is the mean of initial slope of the curves to be compared

$\overline{h}_{20}$ is the mean of the heights of the interfaces of the curves at 20% of the time of the critical point

h_{20i} is the height of interface of i^{th} curve at 20% of the time of the critical point

$\overline{h}_{60}$ is the mean of the heights of the interfaces of the curves at 60% of the time of the critical point

h_{60i} is the height of the interface of the i^{th} curve at 60% of the time of the critical point

$\overline{h}_c$ is the mean of the heights of the interfaces

h_{ci} is the height of the interface of i^{th} curve at the critical point

K is calibration factor

The calibration factor, K, is included in the equation to convert the I_i within a range of 0-100. From the distribution of the results it was found that with K set to a value of 18, 95 out of 100 of the I_i indexes are within 0-100. The calculated I_i, of eight settling curves (shown in Figure 7) resulted from experiments conducted varying flocculant type and dosages, are compared to each other (Table 6).

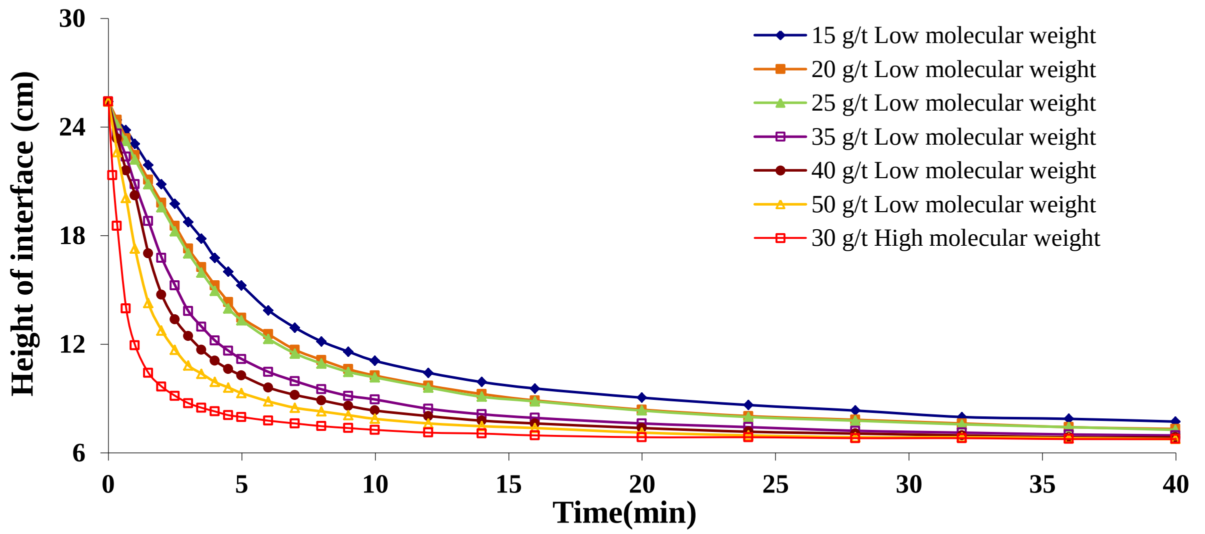

Figure 7. Settling curves of copper tailings resulted from varying flocculant type/dosage, pH=11.3, d_{80}=97 µm.

Table 6. I_i values of settling curves in Fig.7 resulted from varying test conditions

Flocculant dosage (g/t)	Molecular weight type	I_i
15	Low molecular weight	1.32
20	Low molecular weight	2.03
25	Low molecular weight	2.13
35	Low molecular weight	4.69
40	Low molecular weight	8.2
50	Low molecular weight	14.21
30	High molecular weight	78.13

As indicated, an increase in the flocculant dosage leads to an increase in I_i, which can be regarded as an indication of an increase in the settling rate. As can be seen, with the close curves (flocculant dosage 20 and 25 g/t, low molecular weight) the resulted indexes are quiet close.

To focus on a certain part of the settling curves, either the initial settling rates or compression zones are investigated, the contribution of different fractions in Eq. (14) must be differentiated. Clearly, in considering initial settling rate, the final fractions $(\frac{\overline{h_{60}}}{h_{60i}} \times \frac{\overline{h_c}}{h_{ci}})$ are not significant, whereas in studying compression zone, the first fractions $(\frac{S_i}{\overline{S}} \times \frac{\overline{h_{20}}}{h_{20i}})$ are less determinant. Therefore, in Eq. (15), the contribution of different fractions of the tests is regulated by applying coefficients K_1 and K_2.

$$I_i = K_1(\frac{S_i}{\overline{S}} \times \frac{\overline{h_{20}}}{h_{20i}}) + K_2(\frac{\overline{h_{60}}}{h_{60i}} \times \frac{\overline{h_c}}{h_{ci}}) \qquad (15)$$

Where K_1 and K_2 are factors of effectiveness.

The application of presented equations to analyze and compare settling curves is ideal for a computerized approach. Using spread sheets in Microsoft Excel 2007, the computer program "*Batch settling curve analyzer*" (BSCA) on the basis of Eqs. (12, 15), was developed.

4. Conclusion

On the basis of 300 settling experiments performed by varying conditions using iron, copper, coal, lead and zinc, the mathematical model *h(t)* proved to be beneficial in defining a variety of the settling curves, considering R^2 and adjusted R^2 as verification criteria. This model which is a modified version of Banisi and Yahyaei[28] can be used to calculate the settling rate of interface, critical point and initial slope of any settling curve. Results indicated that in very short time after the start of settling tests, settling velocity in most cases reach to a maximum value. In each point the settling rate can be calculated by using the value of the first derivative of *h(t)*. The critical point is located at a point where the second derivative of *h(t)*, is equal to 0.1. Additionally, averaging the values of the first derivative of *h(t)*, for t=0 and t=0.029CPt, results in the initial slope of the settling curve. Furthermore, an index I_i, is introduced and can be used to compare the settling curves quantitatively.

Acknowledgments

The authors would like to thank the National Iranian Copper Industries Company (N.I.C.I.Co.) for supporting this research. Special appreciation is extended to the water supply and metallurgy group of the Shahrebabak Copper Complex. The contribution of R&D division of the (N.I.C.I.Co.), in particular, Mrs. Zeidabadi, is acknowledged. Great appreciation is given to Mr. R. Reza Zade and Miss. M. Hosseini Nasab for their contribution in model verification.

References

[1]. Coe, H.S. and Clevenger, G.H. (1916). Methods for determining the capacities of slime-settling tanks. AIME Transactions 55, 356–384.

[2]. Kynch, C.J. (1952). A theory of sedimentation. Transactions of the Faraday Society 48, 166-176.

[3]. Talmage, W.P. and Fitch, E.B. (1955). Determining thickener unit areas. Industrial and Engineering Chemistry 47, 38–41.

[4]. Fitch, B. (1966). Current theory and thickener design. Industrial and Engineering Chemistry 58, 18-28.

[5]. Wilhelm, J.H. and Naide, Y. (1981). Sizing and operating continuous thickeners, Mining Engineering 33. 1710–1718.

[6]. Merta, H. and Ziolo, J. (1986). Calculation of thickener area and depth based on the data of batch-settling test. Chemical Engineering Science 41, 1918-1920.

[7]. Usher, S.P. (2002). Suspension dewatering: Characterization and optimization. PhD thesis, Department of Chemical Engineering, University of Melbourne, 366p.

[8]. Northcotta, K.A., Snape, I., Scales, P.J. and Stevens, G.W. (2005). Contaminated water treatment in cold regions: an example of coagulation and dewatering modelling in Antarctica. Cold Regions Science and Technology 41, 61– 72.

[9]. Owen, A.T., Fawell, P.D., Swift, J.D. and Farrow, J.B. (2002). The impact of polyacrylamide flocculant solution age on flocculation performance. International Journal of Mineral Processing 67, 123– 144.

[10]. Mpofu, P., Addai-Mensah, J. and Ralston, J. (2004). Flocculation and dewatering behaviour of smectite dispersions: effect of polymer structure type. Minerals Engineering 17, 411–423.

[11]. Nasser, M.S. and James, A.E. (2006). The effect of polyacrylamide charge density and molecular weight on the flocculation and sedimentation behaviour of kaolinite suspensions. Separation and Purification Technology 52, 241–252.

[12]. Addai-Mensah, J. (2007). Enhanced flocculation and dewatering of clay mineral dispersions. Powder Technology 179, 73–78.

[13]. Usher, S.P. and Scales, P.J. (2005). Steady state thickener modelling from the compressive yield stress and hindered settling function. Chemical Engineering Journal 111, 253–261.

[14]. Ekama ,G.A. and Marais, P. (2004). Assessing the applicability of the 1D flux theory to full-scale secondary settling tank design with a 2D hydrodynamic model. Water Research 38, 495–506.

[15]. Garrido, P., Concha, F. and Burger, R. (2003). Settling velocities of particulate systems: 14.Unified model of sedimentation, centrifugation and filtration of flocculated suspensions. International Journal of Mineral Processing 72, 57–74.

[16]. Clauss, F., Helaine, D., Balavoine, C. and Bidault , A. (1998). Improving activated sludge floc structure and aggregation for enhanced settling and thickening performances. Water Science and Technology 38, 35-44.

[17]. Flamant, O., Cockx, A., Guimet, V. and Doquang, Z. (2004). Experimental analysis and simulation of settling process. Process Safety and Environmental Protection 82, 312-318.

[18]. Sanchez, M. (2006). Settling velocity of the suspended sediment in three high-energy environments. Ocean Engineering 33, 665–678.

[19]. Je, C.H., Hayes, D.F., Kim and K.S. (2007). Simulation of resuspended sediments resulting from dredging operations by a numerical flocculent transport model. Chemosphere 70, 187–195.

[20]. Geng, P. and Kuznetsov, A.V. (2005). Settling of bidispersed small solid particles in a dilute suspension containing gyrotactic micro-organisms. International Journal of Engineering Science 43, 992-1010.

[21]. Giokas, D.L., Daigger, G.T., Sperling, M., Kim, Y. and Paraskevas, P.A. (2003). Comparison and evaluation of empirical zone settling velocity parameters based on sludge volume index using a unified settling characteristics database. Water Research 37, 3821–3836.

[22]. Zhang, D., Lia, Z., Lua, P., Zhanga, T. and Xua, D. (2006). A method for characterizing the complete settling process of activated sludge. Water Research 40, 2637 – 2644.

[23]. Takács, I., Patry, G.G. and Nolasco, D. (1991). A dynamic model of the clarification-thickening process. Water Research 25, 1263–1271.

[24]. Cho S.H., Colin F., Sardin M. and Prost, C. (1993). Settling velocity model of activated sludge. Water Research 27, 1237-1242.

[25]. Grijspeerdt, K., Vanrolleghem, P. and Verstraete W. (1995). Selection of one-dimensional sedimentation: Models for on-line use. Water Science and Technology 31, 193-204.

[26]. Watts, R.W., Svoronos S.A. and Koopman B. (1996). One-dimensional modeling of secondary clarifiers using a concentration and feed velocity-dependent dispersion coefficient. Water Research 30, 2112-2124.

[27]. Vanderhasselt, A. and Vanrolleghem, P.A. (2000). Estimation of sludge sedimentation parameters from single batch settling curves. Water Research 34, 395-406.

[28]. Banisi, S. and Yahyaei, M. (2008). Feed dilution based design of a thickener for refuse of a coal preparation plant. Coal Preparation 28, 201-223.

[29]. Grassia, P., Usher, S.P. and Scales, P.J. (2008). A simplified parameter extraction technique using batch settling data to estimate suspension material properties in dewatering applications. Chemical Engineering Science 63, 1971-1986.

[30]. Lester, D.R., Usher S.P. and Scales, P.J. (2005). Estimation of the hindered settling function R(ϕ) from batch-settling tests. AIChE Journal 51, 1158-1168.

[31]. Montgomery, D.C. and Runger, G.C. (2002). Applied statistic and probability for engineers.Third Edition, John Wiley and Sons.

[32]. Garmsiri, M.R. (2008). An investigation into tailings deep cones efficiency improvement at miduk copper complex, M.Sc. dissertation, Shahid Bahonar University of Kerman, Kerman, Iran.

[33]. Gupta, A. and Yan, D.S. (2006). Mineral processing design and operation. Elsevier Science & Technology Books.

[34]. Subramanian, S. and Natarajan, K.A. (1991). Flocculation, filtration and selective flocculation studies on haematite ore fines using starch. Minerals Engineering 4, 587-598.

[35]. Ibrahim, S.S. and Abdel-Khalek, N.A. (1992). The action of different types of corn starch on the flocculation of phosphate slimes. Minerals Engineering 5, 907-916.

[36]. Besra, L., Sengupta, D.K., Roy, S.K. and Ay, P. (2004). Influence of polymer adsorption and conformation on flocculation and dewatering of kaolin suspension. Separation and Purification Technology 37, 231–246.

[37]. van Deventer, B.B.G., Usher, S.P., Kumar, A., Rudman M., Scales, P.J., (2011). Aggregate densification and batch settling. Chemical Engineering Journal 171, 141-151.

[38]. Garmsiri, M.R., Haji Amin Shirazi, H., Yahyaei, M., (2009). Introducing mathematical models to define settling curves in designing thickeners. Twelfth International Seminar on Paste and Thickened Tailings, 129-135.